

Supplementary Materials for

TSHZ2 is an EGF-regulated tumor suppressor that binds to the cytokinesis regulator PRC1 and inhibits metastasis

Mary L. Uribe *et al.*

Corresponding author: Yosef Yarden, yosef.yarden@weizmann.ac.il

Sci. Signal. **14**, eabe6156 (2021)
DOI: 10.1126/scisignal.abe6156

The PDF file includes:

Figs. S1 to S8
Tables S1 to S5
Legend for data file S1
References (68–89)

Other Supplementary Material for this manuscript includes the following:

Data file S1

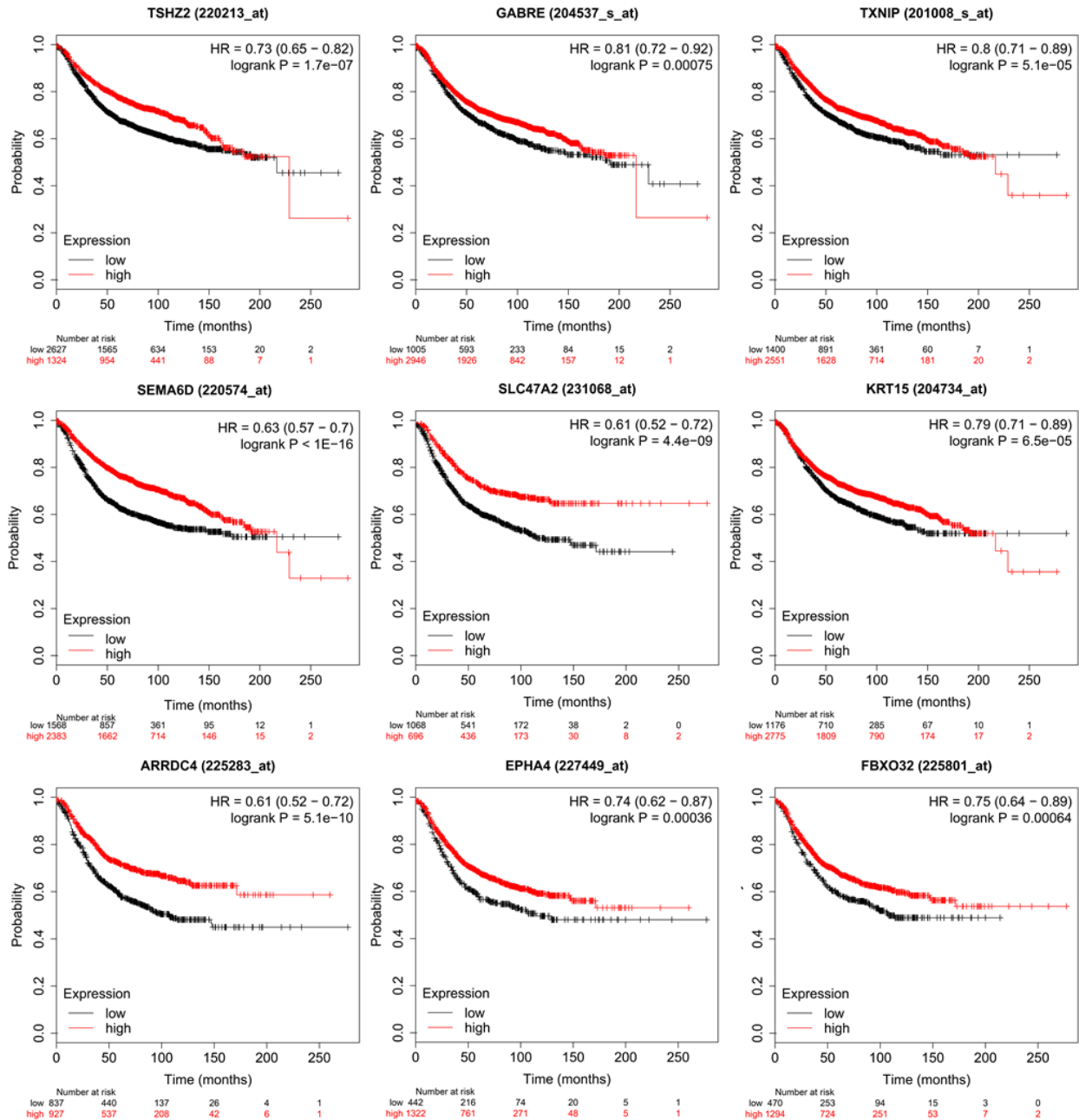


Fig. S1. Transcripts downregulated in response to stimulation of mammary cells with EGF predict longer survival of patients with breast cancer. Kaplan-Meier survival plots, depicting expression levels of specific transcripts and relapse-free survival of patients with breast cancer, are presented. The plots were generated for individual EGF-downregulated transcripts observed in MCF10A cells. The HR, 95% confidence intervals, *P*-values and numbers at risk are displayed on the plots. The Affymetrix IDs are shown. HR, hazard ratio.

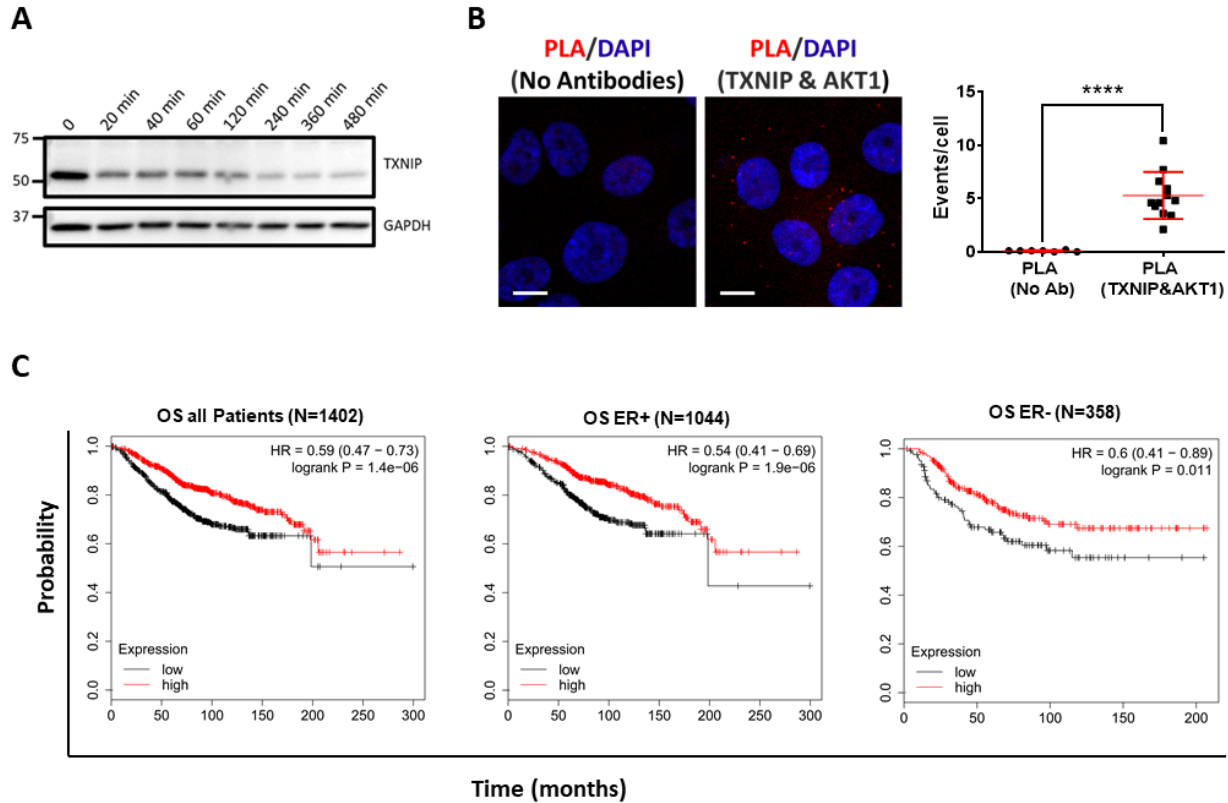


Fig. S2. Downregulation of TXNIP is induced by EGF; lower expression associates with shorter survival of patients with breast cancer. (A) Serum starved MCF10A cells were exposed to EGF as indicated. Cell lysates were subjected to electrophoresis and immunoblotting that used an antibody specific to TXNIP. (B) MCF10 cells pre-seeded in 8-well chamber slides were probed with antibodies recognizing TXNIP and AKT1. Thereafter, the cells were processed for PLA (red signals). Representative images and PLA quantification (averages \pm SEM, $n=3$ experiments) are shown. Scale bar, 20 μ m. Significance was estimated using unpaired t -test with Welch's correction: **** $P < 0.0001$. (C) Kaplan-Meier survival curves presenting the overall survival (OS) of patients with breast cancer according to the KM-plotter web tool. Patients were divided into two equal groups, based on TXNIP levels: low (black) and high (red). Shown are analyses of all patients (left panel), patients with ER-positive tumors (middle panel) or ER-negative tumors (right panel).

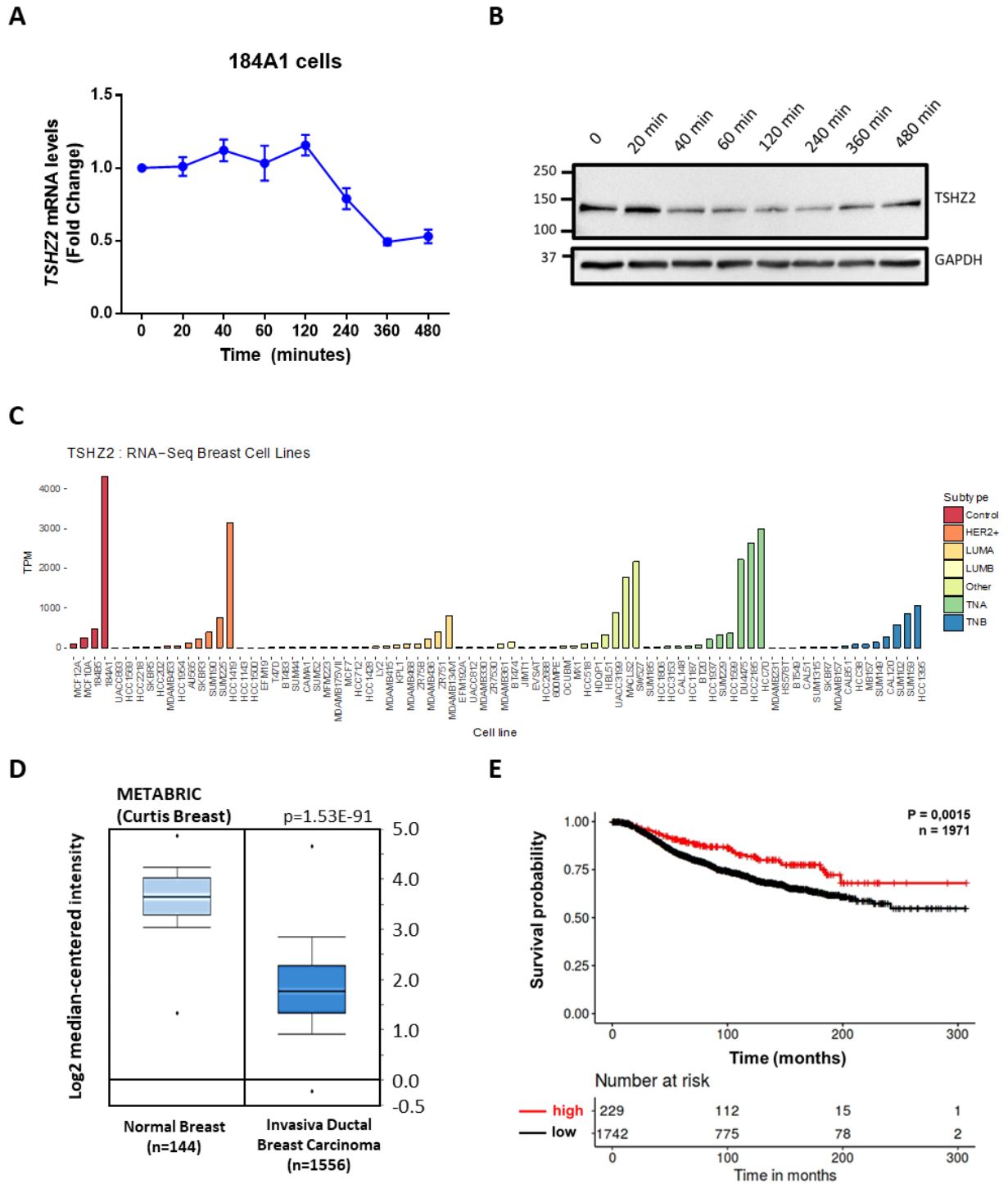


Fig. S3. TSHZ2 is downregulated in an EGF-stimulated mammary cell line; reduced expression predicts shorter survival of patients with breast cancer. (A) mRNA was isolated from 184A1 cells pre-stimulated with EGF for different time intervals. Real-time qPCR was used to quantify the abundance of *TSHZ2* mRNA. Shown are averages \pm SEM (bars), $n=3$. GAPDH mRNA level was used for normalization. (B) Sub-confluent monolayers of 184A1 cells were exposed to EGF (10 ng/ml) for the indicated time intervals. Cell lysates were subjected to gel electrophoresis and immunoblotting that used

an antibody specific to TSHZ2. GAPDH was used as a loading control. (C) Shown are levels of transcripts encoding TSHZ2 in various cell lines of mammary origin (83 cell lines from GEO: GSE73526). In addition to 4 un-transformed cells, the list includes lines derived from the following breast cancer subtypes: luminal A and B, HER2+, triple negative A and B and from other, unidentified origins. (D) Box plot comparing levels of *TSHZ2* mRNA in healthy human breast tissues and ductal breast carcinoma tissues. Data are from METABRIC (68). (E) Kaplan-Meier survival curves presenting the overall survival of patients with breast cancer, according to the METABRIC dataset. Patients were divided into two groups based on *TSHZ2* expression levels: high (red) and low (black). *P*-values, and the numbers of patients are displayed.

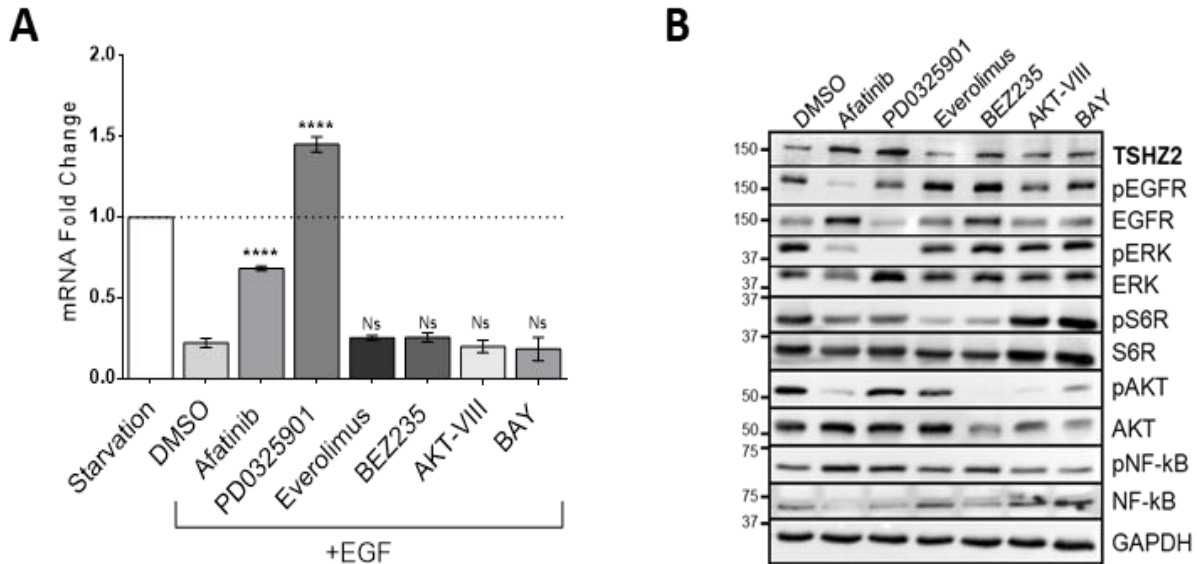


Fig. S4. EGF-induced downregulation of TSHZ2 is mediated by the EGFR-to-MEK signaling pathway. (A and B) MCF10A cells (5×10^5) were seeded in 6-well plates. After 16 hours in starvation medium, the cells were treated for 4 hours with 10 nM Afatinib (EGFR inhibitor), 10nM PD0325901 (MEK inhibitor), 10 nM Everolimus (mTOR inhibitor), 100 nM BEZ235 (PI3K/mTOR inhibitor), 5 μ M AKT1/2 inhibitor (AKT-VIII), or 5 μ M BAY (NF- κ B inhibitor). A solvent control (DMSO) was employed. This was followed by the addition of EGF (10 ng/ml). Cells were washed 18 hours later and both mRNAs and proteins were extracted. Shown in (A) are *TSHZ2* mRNA levels relative to samples treated with starvation medium alone (dotted line). Gene expression was normalized relative to *GAPDH* mRNA levels. The bars represent averages \pm SEM values ($n=4$ experiments). Significance was determined using unpaired *t*-tests: ns, no significance; **** $P < 0.0001$. Proteins were analyzed using immunoblotting with the indicated antibodies (B). Blots are representative of three independent experiments.

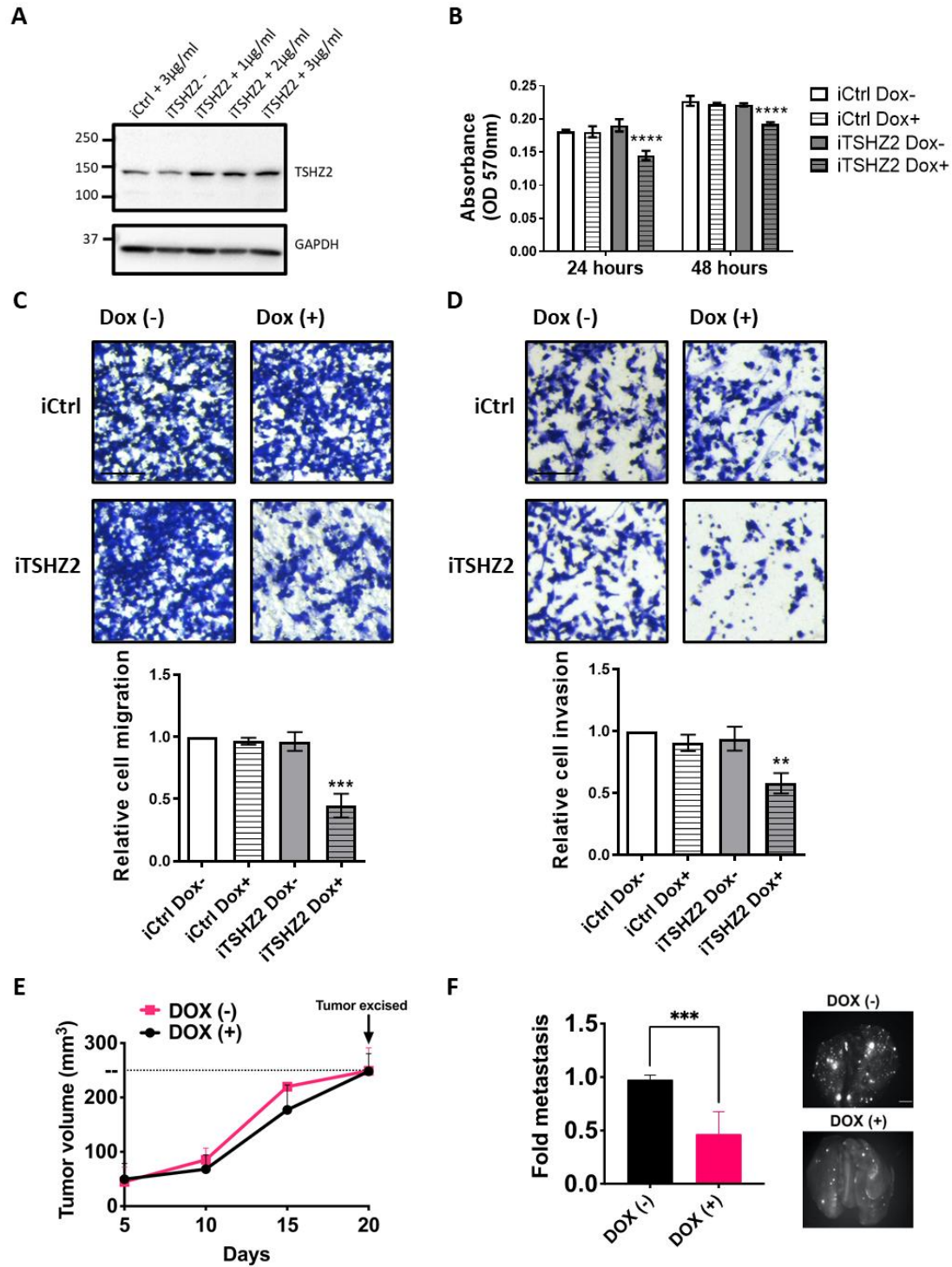


Fig. S5. Inducible overexpression of TSHZ2 decreases growth and motility of MDA-MB-231 cells both in vitro and in vivo. (A) Inducible control MDA-MB-231 cells (iCtrl) and derivatives (iTSHZ2) stably expressing TSHZ2 under control of the tetracycline-inducible mammalian expression system (TRE3G) were exposed to the indicated concentrations of the inducer, doxycycline. Whole cell extracts were immunoblotted with antibodies to either TSHZ2 or GAPDH. (B) MDA-MB-231 cells (10^4 cells/well) were seeded in 96-well plates and later treated for 24 or 48 hours with doxycycline (2 μ g/ml).

Cell viability was assessed using the MTT assay; $n=3$ biological replicates. (C and D) Transwell assays testing migration (C) and invasion (D) of MDA-MB-231 cells, either iCtrl or iTSHZ2, were performed. Cells were treated without or with doxycycline ($2 \mu\text{g/ml}$) sixteen hours prior to the assays. Migrated and invaded cells were fixed and stained with crystal violet (upper panels). Scale bars, $100 \mu\text{m}$. The numbers of migrated and invaded cells were calculated from 4 independent experiments, and they are depicted in the bar charts (lower panel). (E) iTSHZ2 MDA-MB-231 cells (2.5×10^6) were injected into the subaxillary fat pad of female NOG mice ($n=6$ per group). Once individual tumor's size reached 250 mm^3 , it was resected. (F) One day later, animals were treated without or with doxycycline in drinking water, for four weeks. Thereafter, mice were sacrificed, and their lungs were excised and photographed. The bar graph (left panel) presents quantification of lung metastases. Also shown are representative fluorescent lung images. Scale bar, 0.5 cm . All data are shown as mean \pm SEM. Significance was determined using two-way ANOVA with Dunnett's multiple comparison test: $**P < 0.01$, $***P < 0.001$, $****P < 0.0001$.

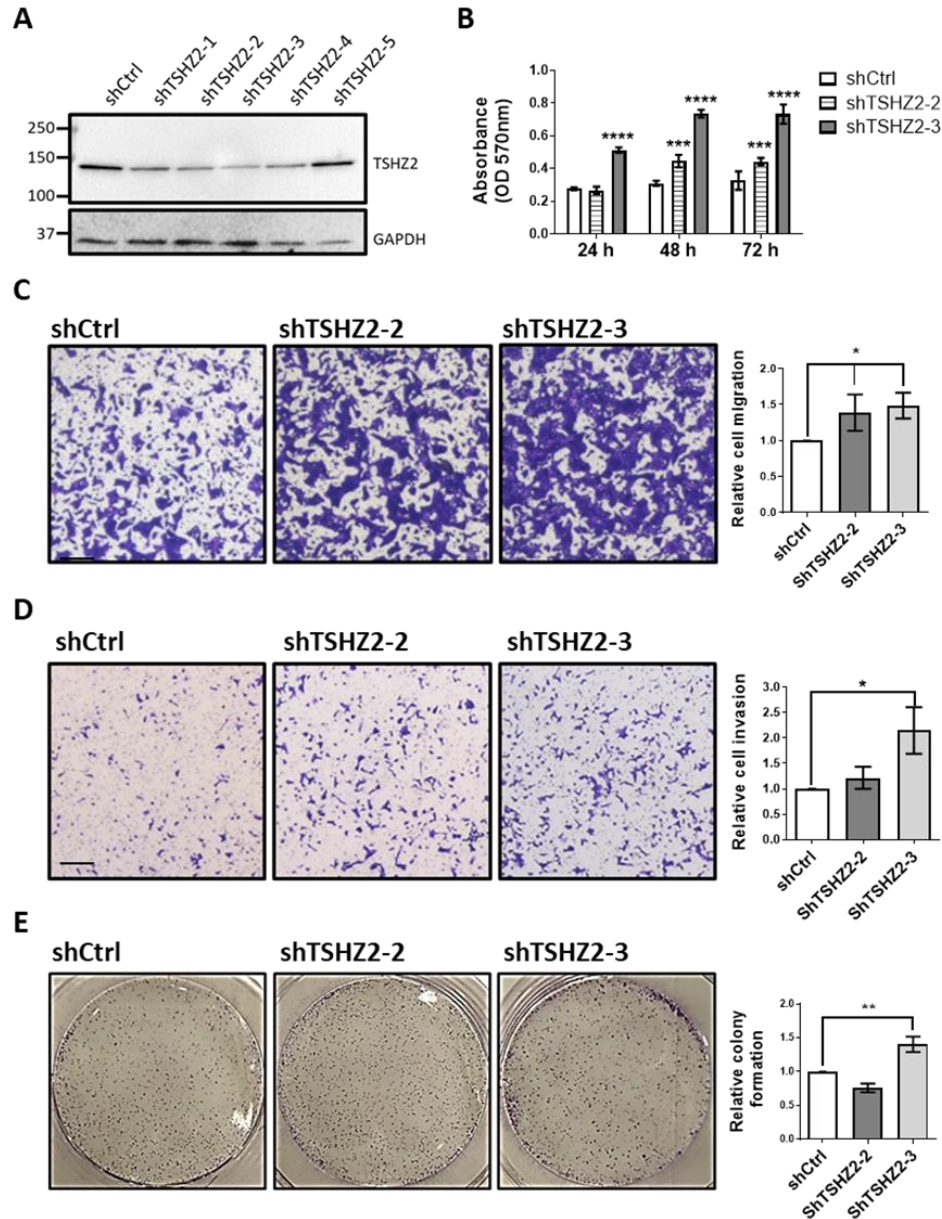
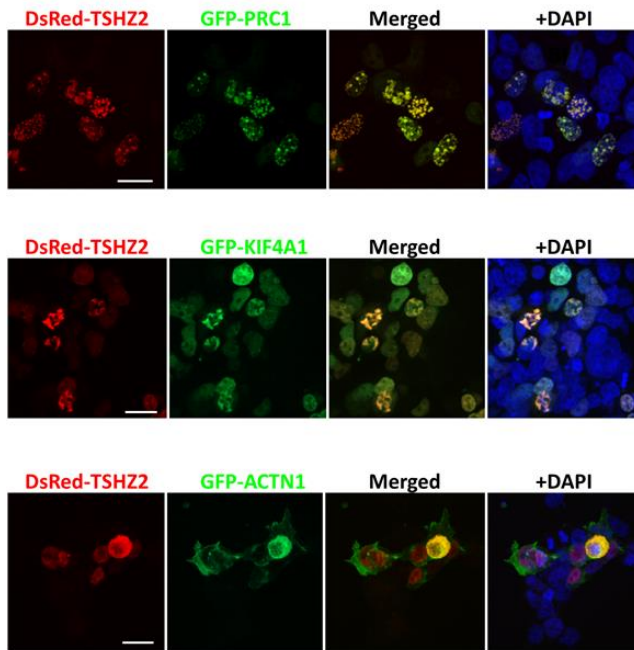


Fig. S6. Silencing *TSHZ2* enhances proliferation, motility, and colony-forming ability of human breast cancer cells. (A) Extracts from HCC70 cells stably expressing 5 different shRNAs specific to *TSHZ2* and scramble control shRNA were immunoblotted using anti-*TSHZ2* and anti-GAPDH antibodies. (B) Three sublines of HCC70 cells, shCtrl, shTSHZ2-2 and shTSHZ2-3 (3×10^4 cells/well) were seeded in 96-well plates. After 24, 48 and 72 hours we determined cell viability using the MTT assay in three biological replicates. (C to E) HCC70 cells presented in B were subjected to migration (C), invasion (D) and clonogenicity (E) assays. For migration and invasion assays, 1×10^5 cells were seeded in migration or invasion chambers. After 18 hours, the migrating or invading cells were fixed and stained with crystal violet. Photos of 5 fields in each chamber were quantified (from four experiments). Scale bars, 0.2 mm. For colony formation assays, HCC70 clones (2×10^3 cells) were plated in 6-well plates and then incubated at 37°C for 7-10 days. Photos of 4 fields in each well were quantified. Data are means \pm SEM of five biological replicates. Significance was determined using two-way ANOVA with Dunnett's multiple comparison test (B) or the Mann-Whitney test (C, D, E): * $P < 0.05$, ** $P < 0.01$, *** $P < 0.001$, **** $P < 0.0001$.

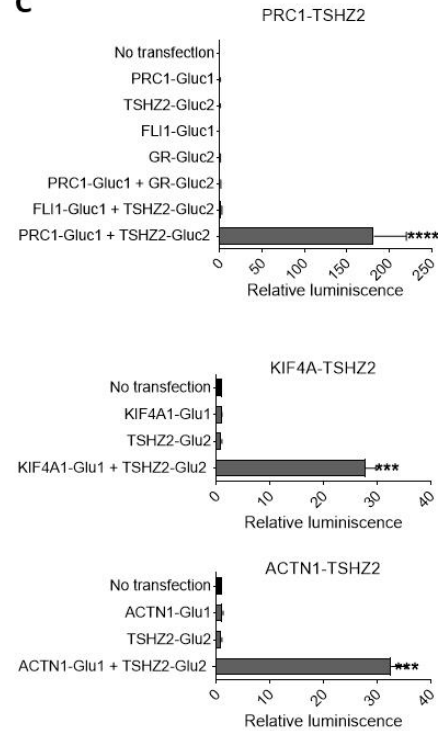
A

Gene symbol	Protein name	Length (aa)	Interaction region	Localization
PRC1	Protein regulator of cytokinesis 1	620	111-275	Nucleus and Cytoskeleton
KIF4A	Chromosome-associated kinesin KIF4A	1232	886-1020	Nucleus and Cytoskeleton
ACTN1	Alpha-actinin-1	892	423-562	Cytoskeleton

B



C



D

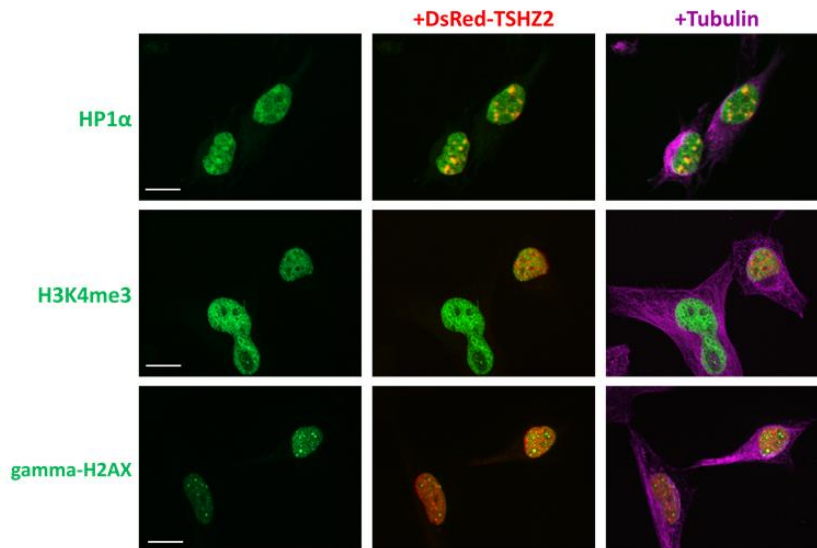


Fig. S7. TSHZ2 physically interacts with PRC1, KIF4A, and ACTN1, as well as localizes with the transcriptionally silenced chromatin. (A) Listed are the top three high-confidence TSHZ2-interacting proteins identified using the yeast two-hybrid screens. (B) HEK293 cells were co-transfected with

plasmids encoding DsRed-TSHZ2 and either GFP-PRC1, GFP-KIF4A or GFP-ACTN1. Thereafter, cells were seeded in round bottom glasses and prepared for immunofluorescence. The slides were viewed in a spinning disc microscope. Nuclei were stained with DAPI. Scale bars, 20 μ m. (C) Protein complementation assays (PCA) tested physical interactions between the following pairs: TSHZ2-PRC1, TSHZ2-KIF4A and TSHZ2-ACTN1. The amino-terminal segment (Gluc1) of the Gaussia luciferase protein was fused to PRC1, KIF4A, ACTN1 or FLI1 (negative control), whereas the carboxyl-terminal segment (Gluc2) was fused to TSHZ2 or GR (negative control). The assay was performed in HEK293T cells (6×10^3), which were un-transfected, pre-transfected with each Gluc plasmid alone, or with combinations of the Gluc1 and Gluc2 plasmids. Forty-eight hours post-transfection, we measured luciferase activity using a luminescence plate reader. Shown are normalized luciferase signals \pm SD from three independent experiments. Significance was assessed using one-way ANOVA with Dunnett's multiple comparison test: **** $P < 0.0001$, *** $P < 0.001$. (D) HeLa cells pre-transfected with DsRed-TSHZ2 expression vector were labeled with antibodies against endogenous HP1 α , H3K4me3 or gamma-H2AX (phospho-histone H2AX). An anti-tubulin antibody was used as counterstain. Analysis of the green, red, and merged fluorescence was performed with a confocal microscope. Scale bar, 20 μ m.

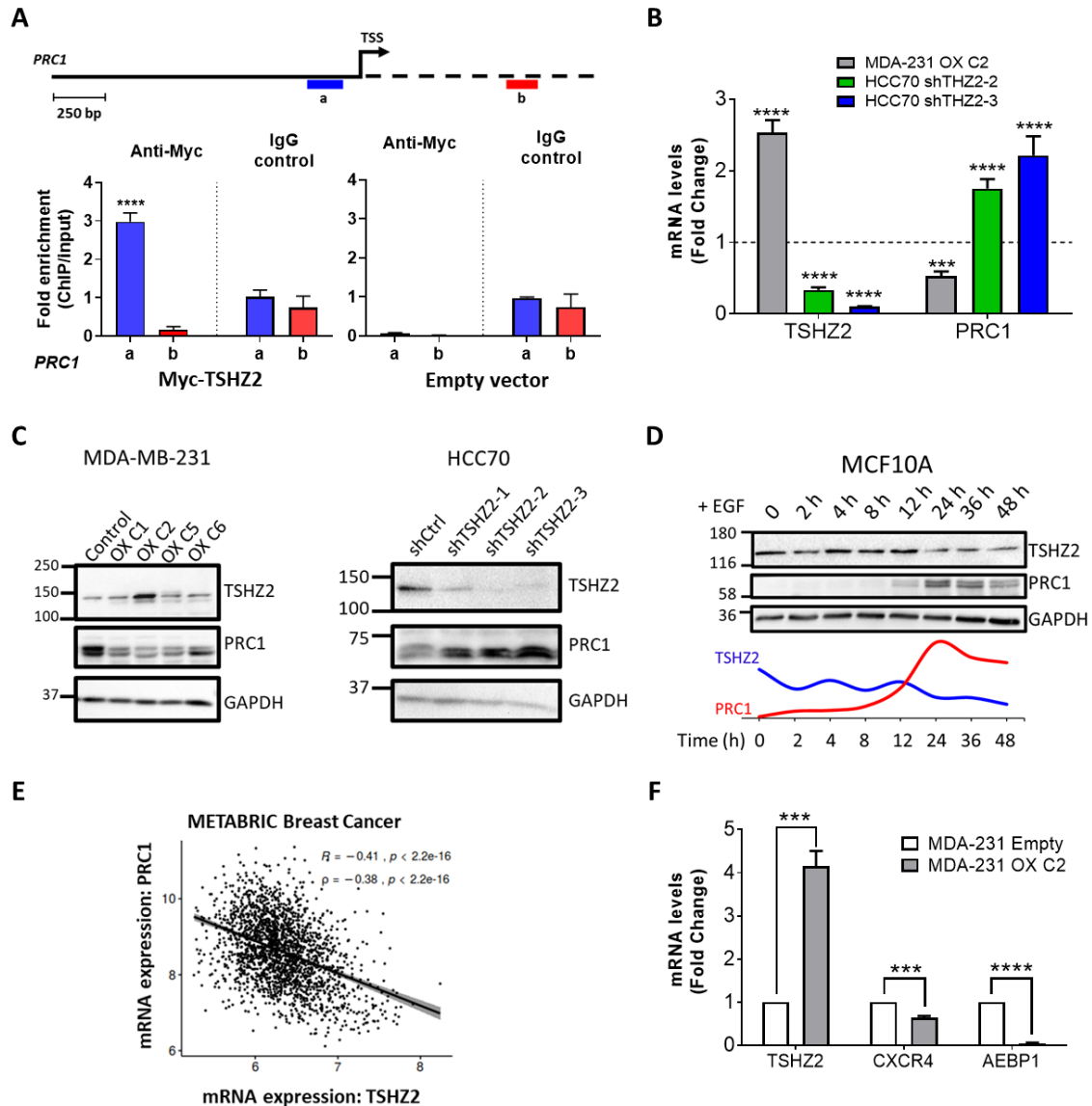


Fig. S8. TSHZ2 transcriptionally represses PRC1 and two GLI1 target genes. (A) HEK293T cells were transfected with a MYC-tagged TSHZ2 plasmid, or with an empty vector. After 48 hours, complexes containing cross-linked chromatin and fragments of genomic DNA were pulled down using an anti-MYC antibody, or control IgG. The complexes were subjected to qPCR reactions using primers targeting either a region upstream to the transcription start site (TSS) (a; in blue) or an intragenic region (b; in red). The schematic diagram shows the location of each primer we used, relative to the TSS (upper panel). Amplicon a: nucleotides -253 to -86; amplicon b: +681 to +832. Each qPCR reaction was repeated three times in two independent experiments. Data show means \pm SD (lower panels). (B) mRNA was isolated from MDA-MB-231 cells overexpressing TSHZ2 (OX C2) and HCC70 cells that were pre-treated with the indicated TSHZ2-specific shRNAs. Real-time qPCR was used to quantify the abundance of PRC1's mRNA along with TSHZ2's mRNA. Shown are mRNA levels relative to the respective parental cells. Shown are means \pm SEM of three different experiments. The dotted line refers to the parental control cells. (C) Whole extracts from MDA-MB-231 cells stably overexpressing TSHZ2 (left panel), along with *TSHZ2* knocked-down HCC70 cells (right panel) were immunoblotted using antibodies specific to TSHZ2, PRC1 and GAPDH, which served as a marker of equal gel loading. (D) Cell extracts

from MCF10A cells pre-stimulated with EGF for the indicated time intervals were immunoblotted using antibodies specific to TSHZ2 or PRC1. Bands were quantified using densitometry and signals were normalized to GAPDH (bottom panel). (E) Scatter plot of PRC1 and TSHZ2 expression levels in mammary tumors (according to METABRIC dataset). The correlation was calculated using the Pearson (R) and Spearman (“rho”) coefficients. (F) Transcript levels of two GLI1 target genes, CXCR4 and AEBP1, were analyzed using RT-qPCR, and mRNA isolated from both C2 cells and parental cells (denoted *Empty*). GAPDH mRNA levels were used for normalization. Data are means \pm SEM of three independent experiments. Significance was assessed using two-way ANOVA with Sidak's multiple comparisons test (A), Dunnett's multiple comparison test (B) or multiple *t*-test with the Bonferroni-Dunn method (F): *** $P < 0.001$, **** $P < 0.0001$.

#	Gene	#	Gene	#	Gene	#	Gene	#	Gene
1	<i>FBXO32</i>	21	<i>EEF2K</i>	41	<i>TBC1D3C</i>	61	<i>PBX1</i>	81	<i>VANGL2</i>
2	<i>KRT15</i>	22	<i>SEMA6D</i>	42	<i>TBC1D3L</i>	62	<i>ZNF608</i>	82	<i>SYNPO</i>
3	<i>ARRDC4</i>	23	<i>ABHD4</i>	43	<i>TBC1D3H</i>	63	<i>DLEU2</i>	83	<i>CALCOCO1</i>
4	<i>SLC47A2</i>	24	<i>PIK3C2B</i>	44	<i>TBC1D3D</i>	64	<i>PELI2</i>	84	<i>IMPA2</i>
5	<i>NUMA1</i>	25	<i>TSHZ2</i>	45	<i>TBC1D3E</i>	65	<i>DDB2</i>	85	<i>DLEU2L</i>
6	<i>TXNIP</i>	26	<i>NOTCH1</i>	46	<i>TBC1D3G</i>	66	<i>CYP4F12</i>	86	<i>IFIT2</i>
7	<i>GABRE</i>	27	<i>INPPL1</i>	47	<i>TBC1D3B</i>	67	<i>ID3</i>	87	<i>Z83843.1</i>
8	<i>CHD6</i>	28	<i>PIK3IP1</i>	48	<i>GCLC</i>	68	<i>ATF7IP</i>	88	<i>RN7SL648P</i>
9	<i>UGT1A5</i>	29	<i>MEGF9</i>	49	<i>FXRD3</i>	69	<i>FIBIN</i>	89	<i>CDKN1B</i>
10	<i>EPHA4</i>	30	<i>FAM111A</i>	50	<i>LAMA5</i>	70	<i>UGT1A3</i>	90	<i>KITLG</i>
11	<i>CYP11B1</i>	31	<i>UBE2Q2P6</i>	51	<i>FGFR2</i>	71	<i>IRX5</i>	91	<i>KLHL31</i>
12	<i>MAF</i>	32	<i>LCAL1</i>	52	<i>STAG3L5P</i>	72	<i>PIK3C2G</i>	92	<i>OR9A4</i>
13	<i>ZSCAN31</i>	33	<i>LDB1</i>	53	<i>H4C15</i>	73	<i>ATP1B3</i>	93	<i>TMEM78</i>
14	<i>HS6ST1P1</i>	34	<i>TBC1D3J</i>	54	<i>CUTALP</i>	74	<i>ATP6V0CP4</i>	94	<i>RN7SKP24</i>
15	<i>GATA3</i>	35	<i>TBC1D3I</i>	55	<i>TBC1D3P1</i>	75	<i>YPEL2</i>	95	<i>ZNF546</i>
16	<i>KLHL24</i>	36	<i>TBC1D3F</i>	56	<i>SESN3</i>	76	<i>RPS4XP16</i>	96	<i>RN7SKP168</i>
17	<i>ABCC2</i>	37	<i>TBC1D3K</i>	57	<i>H4C14</i>	77	<i>CA2</i>	97	<i>RAB30</i>
18	<i>RIPK4</i>	38	<i>SRGAP2C</i>	58	<i>MRI</i>	78	<i>RNA5SP107</i>	98	<i>OR56A1</i>
19	<i>UBE2Q2L</i>	39	<i>EID3</i>	59	<i>KSRI</i>	79	<i>BCL11A</i>	99	<i>RN7SL515P</i>
20	<i>UGT1A4</i>	40	<i>TBC1D3</i>	60	<i>TBC1D3P2</i>	80	<i>CPEB3</i>	100	<i>ERVK9-11</i>

Table S1. List of the top 100 delayed downregulated genes (DDGs). Differential expression analysis was performed using data extracted from the GSE24391 dataset. Genes downregulated at least one limit fold change (LFC) with a *P*-value < 0.05 (for each time point), were initially selected. Thereafter, all genes that showed persistent downregulation in at least two consecutive time points were retained, while genes that showed any upregulation after the 20 minutes time point were excluded. Shown are all top 100 genes ranked according to the significance of their downregulation after EGF treatment for 240 and 480 min.

<i>Gene</i>	<i>Short name</i>	<i>NCBI gene ID</i>	<i>Description</i>	<i>Relevance to cancer and complex formation with oncoproteins</i>	<i>Ref</i>
<i>F-box protein 32</i>	<i>FBXO32</i>	114907	An F-box protein family member of ubiquitin ligases called SCFs (SKP1-cullin-F-box).	Downregulated in cancer via promotor hypermethylation. Sorts KLF4 for ubiquitination and degradation.	(13, 69)
<i>Keratin 15</i>	<i>KRT15</i> (CK15)	3866	A member of the keratin gene family. Responsible for the structural integrity of epithelial cells.	Downregulated in breast cancer and gastric cancer (GC). The gene is hyper-methylated in gastric cancer and associates with overall patient survival.	(70)
<i>Cyclin dependent kinase inhibitor 1B</i>	<i>CDKN1B</i> (p27)	1027	A protein inhibitor of two cyclin-dependent kinases.	Low levels correlate with metastasis and shorter survival of patients with breast cancer. Binds to and prevents the activation of cyclin E-CDK2 and cyclin D-CDK4 complexes.	(71)
<i>Phosphoinositide-3-kinase interacting protein 1</i>	<i>PIK3IP1</i>	113791	Negative regulator of PI3K activity.	Acts as a tumor suppressor when Ras is activated. Binds to and inhibits PI3K.	(72)
<i>Gamma-aminobutyric acid type A receptor subunit epsilon</i>	<i>GABRE</i>	2564	The receptor of the main inhibitory neurotransmitter in the adult brain.	The <i>GABRE</i> /miR-452/miR-224 locus is epigenetically silenced in prostate cancer.	(73)
<i>Arrestin domain containing 4</i>	<i>ARRDC4</i>	91947	Recruits ubiquitin ligases that mediate endocytosis of activated G protein-coupled receptors.	<i>ARRDC4</i> is frequently methylated in patients with gastric cancer. High <i>ARRDC4</i> levels predict better prognosis of patients with breast cancer.	(74, 75)
<i>Solute carrier family 47 member 2</i>	<i>SLC47A2</i> (MATE2)	146802	A transporter involved in excretion of toxic electrolytes.	Epigenetically repressed in kidney cancer.	(76)
<i>Calcium binding and coiled-coil domain 1</i>	<i>CALCOCO1</i>	57658	Physically interacts with MAP1LC3C, a key player of autophagy. Deletion of <i>CALCOCO1</i> disrupted reticulophagy.	Regulated by miR-574-5p and lncRNA LINC00052. Downregulated in colorectal cancer.	(77, 78)
<i>UDP glucuronosyltransferase family 1 member A4 & A5</i>	<i>UGT1A4</i> & <i>UGT1A5</i>	54657 & 54579	Transforms small lipophilic molecules, such as steroids, and drugs, into excretable metabolites.	<i>UGT1A5</i> 's mRNA was found to be downregulated in stomach cancer.	(79)
<i>Thioredoxin interacting protein</i>	<i>TXNIP</i>	10628	A member of the alpha arrestin family. Inhibits the antioxidative function of thioredoxin.	A novel tumor suppressor in thyroid cancer. Binds and inhibits thioredoxin and AKT.	(34, 80)
<i>Semaphorin 6D</i>	<i>SEMA6D</i>	80031	Belongs to a family of secreted and membrane proteins acting as inhibitors or chemorepellents in axon pathfinding.	High <i>SEMA6D</i> predicts longer survival of patients with breast cancer.	(14)

<i>Receptor interacting serine/threonine kinase 4</i>	<i>RIPK4</i>	54101	Interacts with protein kinase C-delta. Can also activate NF-kappa-B.	Downregulated in bone metastases of breast cancer. A putative tumor suppressor in hepatocarcinogenesis.	(81, 82)
<i>GATA binding protein 3</i>	<i>GATA3</i>	2625	Belongs to the GATA family of transcription factors.	Inhibits breast tumors and metastasis through the regulation of metastasis-associated genes.	(83)
<i>Teashirt zinc finger homeobox 2</i>	<i>TSHZ2</i>	128553	A transcription repressor containing a homeobox DNA-binding domain and a coiled-coil domain.	Downregulated in breast and prostate cancer. Binds with PRC1, KIF4A and alpha-actinin (reported herein).	(19, 20)
<i>EPH receptor A4</i>	<i>EPHA4</i>	2043	A receptor tyrosine kinase; binds membrane-bound ephrin family ligands.	-Reduced in invasive breast cancer. EPHA4 expression is associated with an improved outcome in patients with resected lung adenocarcinoma.	(84, 85)
<i>Eukaryotic elongation factor 2 kinase</i>	<i>EEF2K</i>	29904	A highly conserved protein kinase in the calmodulin-mediated signaling pathway. Involved in the regulation of protein synthesis.	Functions as cancer suppressor in lung cancer cells. Forms a complex with PKM2 and STAT3, and blocks cell proliferation by inactivation of STAT3 and MYC.	(86)
<i>Abhydrolase domain containing 4, N-acyl phospholipase B</i>	<i>ABHD4</i>	63874	Lysophospholipase selective for N-acyl phosphatidylethanolamine (NAPE).	A p53-target gene. ABHD4 knockdown confers resistance to anoikis.	(87)
<i>Nuclear mitotic apparatus protein 1</i>	<i>NUMA1</i>	4926	A microtubule binding component of the nuclear matrix. Regulates mitotic spindle formation. Binds with P53-binding protein 1 (53BP1).	Binds p53 following DNA damage and regulates p53-mediated transcription. High NUMA1 expression associates with patient survival gain in breast cancer.	(88, 89)

Table S2. List of selected DDGs, along with their relevance to cancer. Listed and described are 19 genes selected from table S1 for their relevance to cancer.

PBS	Gene	PBS	Gene	PBS	Gene	PBS	Gene	PBS	Gene
A	<i>PRC1</i>	D	<i>ANKRD18B</i>	D	<i>GCC2</i>	D	<i>LNPEP</i>	D	<i>TRIM47</i>
	<i>KIF4A</i>		<i>APLP2</i>		<i>GOLGA2</i>		<i>MYO5B</i>		<i>TRIM59</i>
	<i>ACTN1</i>		<i>BTBD2</i>		<i>GOLGA3</i>		<i>PCM1</i>		<i>TRIP11</i>
	<i>ZNF451</i>		<i>C20orf117</i>		<i>GPSM2</i>		<i>PCNT</i>		<i>UACA</i>
B	<i>CCNB1</i>		<i>CCDC18</i>		<i>GTF3C2</i>		<i>RABEP1</i>		<i>UBXD5</i>
	<i>DCTN1</i>		<i>CCHCR1</i>		<i>IPO5</i>		<i>RINT1</i>		<i>UHMK1</i>
	<i>IMMT</i>		<i>CDC42BPB</i>		<i>KDM5B</i>		<i>RNF40</i>		<i>VCPIP1</i>
	<i>MCM3AP</i>		<i>CENPF</i>		<i>KIAA1586</i>		<i>RORC</i>		<i>VPS39</i>
	<i>NUP155</i>		<i>CEP152</i>		<i>KIF11</i>		<i>SLX4</i>		<i>VPS54</i>
	<i>ODF2</i>		<i>CEP57</i>		<i>KIF3C</i>		<i>SNX1</i>		<i>ZNF202</i>
	<i>SYNE2</i>		<i>CIT</i>		<i>KLC2</i>		<i>SPAG5</i>		
	<i>TRIM37</i>		<i>CNTROB</i>		<i>KPNA2</i>		<i>SRGAP3</i>		
	<i>TRIO</i>		<i>COG6</i>		<i>KPNA3</i>		<i>TERF1</i>		
	<i>TUBGCP4</i>	<i>CROCC</i>	<i>KRT19</i>	<i>TFIP11</i>					
	<i>UBE4A</i>	<i>DSP</i>	<i>KRT80</i>	<i>TLN2</i>					
C	<i>EDC4</i>	<i>ENOX2</i>	<i>LAMA5</i>	<i>TPR</i>					
	<i>MACF1</i>	<i>EPS8L2</i>	<i>LIMD1</i>	<i>TRIM29</i>					
	<i>PCMT1</i>	<i>FLOT1</i>	<i>LMNB2</i>	<i>TRIM45</i>					

Table S3. List of putative partners of TSHZ2 revealed using yeast 2-hybrid screens. The cDNA of TSHZ2 (amino acids 36-1034) was cloned as a C-terminal fusion partner of LexA (N-LexA-TSHZ2-C fusion). This construct was used as a bait to screen a random-primed human breast tumor epithelial cell cDNA library. Candidates are grouped according to their Predicted Biological Score (PBS), from A to D.

Gene/ plasmid	Primer sequence
<i>TSHZ2</i>	Fw: 5'-AGGCGCTACCTGTTTGAAGAA -3'
	Rv: 5'-GCTTCTGAGGTGGGGACATA-3'
<i>GABRE</i>	Fw: 5'-TCGTATCAATAGCCGTGCCC -3'
	Rv: 5'-CAGGCGGTAGACATGGATGC -3'
<i>TXNIP</i>	Fw: 5'-CTGGCGTAAGCTTTTCAAGG -3'
	Rv: 5'-AGTGCACAAAGGGGAAACAC -3'
	Rv: 5'-AGTGAAGGTGAGGCCCTTGAAG-3'
<i>GAPDH</i>	Fw: 5'-GGGTCATTGATGGCAAC-3'
	Rv: 5'-GAAGGTGAAGGTTCGGA-3'
<i>PRC1</i>	Fw: 5'-TAGACCACACCCAGACACAAG-3'
	Rv: 5'-CCCCTCACACACTGCTTCATT-3'
<i>CXCR4</i>	Fw: 5'-TGTTGGCTGAAAAGGTGGTC-3'
	Rv: 5'-AAAGATGAAGTCGGGAATAGTC-3'
<i>AEBP1</i>	Fw: 5'-AGACCACGCCATCTTCCG-3'
	Rv: 5'-CCTTGTGTTCTCCCACTCG-3'
<i>mTshz2</i>	Fw 5'-GTGAGACTGGAGCTAAGTAGAGC-3'
	Rv: 5'-TGGAGGCTGTAGAACTCTGC-3'
<i>PRC1-a</i>	Fw 5'-ATTTTCTTGGAGCGACGGGA-3'
	Rv: 5'-TCCAGACCTACTCCACACGG -3'
<i>PRC1-b</i>	Fw 5'-TAGACCACACCCAGACACAAG -3'
	Rv: 5'-CCCCTCACACACTGCTTCATT-3'
PRC1- GLUC1	Fw: 5'-AGCACAGTGGCGGCCGCATGAGGAGAAGTGAGGTGCT-3'
	Rv: 5'-CCACCGCCACCATCGATGGACTGGATGTTGGTTGAAT-3'
KIF4A- GLUC1	Fw: 5'-AGCACAGTGGCGGCCGCATGAAGTTTAGACAGTGGAAGCA-3'
	Rv: 5'-CCACCGCCACCATCGATGTGGGCTCTTCTTCGATAGG-3'
ACTN1- GLUC1	Fw: 5'-AGCACAGTGGCGGCCGCATGGACCATTATGATTCTCA-3'
	Rv: 5'-CCACCGCCACCATCGATGAGGTCACTCTCGCCGTACA-3'
FLI1 GLUC1-	Fw: 5'-AGCACAGTGGCGGCCGCATGGACGGACTATTAAGGAGGCTCTGTTCG-3'
	Rv: 5'-CCACCGCCACCATCGATCTAGTAGTAGCTGCCTAAGTGTGAAGGC-3'
GR-GLUC2	Fw: 5'-AGCACAGTGGCGGCCGCATGGACTCCAAGAATCATTAACTCCTGGTA-3'
	Rv: 5'-CCACCGCCACCATCGATCTTTTATGAAACAGAAGTTTTTTGATATTCC-3'
TSHZ2- GLUC2	Fw: 5'-AGCACAGTGGCGGCCGCATGCCGAGGAGAAAACAGCA-3'
	Rv: 5'-CCACCGCCACCATCGATTTCTTCATCCACGTCTGTTA-3'
pSpCas9 (<i>mTshz2</i>)	Fw: 5'-CACCGCAGTGC GGCTACGACACTCTCG -3'
	Rv: 5'-AAACCGAGAGTGTCTGATAGCCGCACTGC -3'

Table S4. List of primers used for qRT-PCR and cloning. Fw, forward primer; Rv, reverse primer.

Antibody (clone)	Source	Identifier	Host
TSHZ2	BioVision	A1171	Rabbit
TSHZ2	LSBio	LS-C201262	Rabbit
GAPDH	Merck	MAB374	Mouse
α/β -Tubulin	Cell Signaling Technology	2148	Rabbit
α -Tubulin (DM1A)	Cell Signaling Technology	3873	Mouse
BrdU-FITC (BU20A)	Thermo Fisher Scientific	11-5071-41	Mouse
c-Myc (9E10)	Santa Cruz Biotechnology	sc-40	Mouse
PRC1 [T481] (EP1514Y)	Abcam	ab62366	Rabbit
PRC1	Aviva Systems Biology	OAA02101	Rabbit
KIF4A	Aviva Systems Biology	OAGA05174	Rabbit
Cyclin B1 (D5C10)	Cell Signaling Technology	12231	Rabbit
p27 Kip1 (D69C12)	Cell Signaling Technology	3686	Rabbit
Cyclin A2 (BF683)	Cell Signaling Technology	4656	Mouse
HA-Tag (C29F4)	Cell Signaling Technology	3724	Rabbit
TXNIP (VDUP1)	MLB International	K0205-3	Mouse
AKT1 (C73H10)	Cell Signaling Technology	2938	Rabbit
pEGF [Tyr ¹⁰⁶⁸]	Cell Signaling Technology	2234	Rabbit
EGF (D38B1)	Cell Signaling Technology	4267	Rabbit
pErk1/2 [Thr ²⁰² /Tyr ²⁰⁴]	Cell Signaling Technology	9101	Rabbit
Erk1/2 (137F5)	Cell Signaling Technology	4695	Rabbit
pS6R [Ser ^{240/244}] (D68F8)	Cell Signaling Technology	5364	Rabbit
S6R (5G10)	Cell Signaling Technology	2217	Rabbit
pAkt [Ser ⁴⁷³] (D9E)	Cell Signaling Technology	4060	Rabbit
pNF- κ B p65 [Ser ⁵³⁶] (93H1)	Cell Signaling Technology	3033	Rabbit
NF- κ B p65 (L8F6)	Cell Signaling Technology	6956	Mouse
HP1 α	Cell Signaling Technology	2616	Rabbit
H3K4me3 (C42D8)	Cell Signaling Technology	9751	Rabbit
Gamma-H2AX [Ser ¹³⁹]	Cell Signaling Technology	2577	Rabbit

Table S5. List of all primary antibodies used in this study.

Data file S1. Yeast two-hybrid screen data.